

Galactic chemical evolution in hierarchical formation models - II. The Intracluster Medium.

Matías Arrigoni^{1*}, Scott C. Trager¹ and Rachel S. Somerville^{2,3}

¹*Kapteyn Astronomical Institute, University of Groningen, Postbus 800, NL-9700 AV Groningen, The Netherlands*

²*Space Telescope Science Institute, 3700 San Martin Drive, Baltimore, MD 21218, USA*

³*Department of Physics and Astronomy, Johns Hopkins University, Baltimore, MD 21218, USA*

Accepted . Received .

ABSTRACT

We use the cosmological semi-analytic model (SAM) for galaxy formation presented in Paper I to study the metallicities and abundance ratios of the intracluster medium (ICM) within the hierarchical structure formation paradigm. By requiring a slightly flat IMF ($x = 1.15$) and a two-population delay-time-distribution (DTD) for SN Ia explosions we found previously that this model is able to reproduce the abundance ratios and supernova rates of early-type galaxies in the local Universe. Predictions for elemental abundances in the ICM pose a further test of the model. We find that with the fiducial model from Paper I the overall metal content of the ICM is too low, although the abundance ratios are in good agreement with the data. However, we find that allowing a fraction of the metal-enriched material ejected by stars to be deposited directly into the hot ICM, instead of being deposited into the cold ISM, appears to be a plausible and physically-motivated solution.

Key words: galaxies: clusters: general – galaxies: clusters: intracluster medium – galaxies: abundances – galaxies: evolution – galaxies: formation

1 INTRODUCTION

The vast majority of baryons in the Universe reside not in stars but in the hot and diffuse gas in clusters of galaxies—the intracluster medium (ICM)—which provides the fuel for star formation in galaxies (e.g. Lin et al. 2003; Vikhlinin et al. 2006). The metal content in this gas suggests that it cannot be entirely of primordial origin and that a substantial fraction must have been processed by the cluster galaxies and then expelled back into the ICM via supernovae explosions and galactic winds. This interplay between the ICM and galaxies regulates the star formation and enrichment histories (Renzini 1997) of the Universe. Measurement of elemental abundances in clusters can therefore set constraints on the various feedback processes that shape galaxy formation, as well as the relative importance of different types of supernovae and the history of star formation. Any successful model of galaxy formation must account not only for the observational properties of the galaxy population but also those of the ICM.

The intergalactic medium within groups and clusters is hot and dense enough to be observed at X-ray wavelengths. At these wavelengths Fe is the most easily observ-

able element. The X-ray satellites launched since the mid-90's (ASCA, BeppoSax, Chandra, XMM-Newton) have allowed precise measurements of many other elements such as O, Mg, Si, S, Ar, Ca and Ni in large samples of nearby clusters (Fukazawa et al. 1998; Peterson et al. 2003; De Grandi et al. 2004; Tamura et al. 2004; de Plaa et al. 2007). As with early-type galaxies, most of the chemical modelling of the ICM has been done within the monolithic collapse scenario (Matteucci & Gibson 1995; Gibson & Matteucci 1997); only a handful of studies have been carried out within the hierarchical assembly paradigm (De Lucia et al. 2004; Nagashima et al. 2005a). These models, however, have their own limitations. De Lucia et al. (2004) assume the instantaneous recycling approximation and trace only the total metallicity and enrichment by type II supernovae (SNe II). Nagashima et al. (2005a), on the other hand, fully couple galactic chemical evolution models to a SAM and successfully reproduce the abundances of various elements in the ICM, but the same model predicts incorrect trends of stellar abundance ratios in the early-type galaxies within those clusters (Nagashima et al. 2005b).

In this work, we continue our study of galactic chemical evolution hierarchical assembly models of galaxy formation within a Λ CDM cosmology (Arrigoni et al. 2010, hereafter Paper I), by studying the metallicity and abundance ratios

* email: arrigoni@astro.rug.nl

of the hot intracluster gas. The outline of the paper is as follows. In Section 2 we briefly describe the semi-analytic model and the new ingredients. In Section 3 we present our predictions and compare them with observations. In Section 4 we summarise our findings and present our conclusions.

2 THE SEMI-ANALYTIC MODEL

The backbone of our model is the SAM described by Somerville et al. (2008, hereafter S08), which tracks the hierarchical clustering of dark matter haloes, radiative cooling of gas, star formation, SN feedback, AGN feedback (in two distinct modes, quasars and radio jets), galaxy mergers and the starbursts triggered by them, the evolution of stellar populations, and the effects of dust obscuration. In Paper I, we described our extension of this model to include detailed metal enrichment by type Ia and type II supernovae and long-lived stars. We refer the reader to the two aforementioned studies for a detailed description of the models.

The SAM has been successful in reproducing a variety of observations in the local Universe and at high redshift, for example, the luminosity and stellar mass function of galaxies, the colour–magnitude relation, galaxy star formation rates as a function of their stellar masses, the relative numbers of early and late-type galaxies, the gas fractions and size distributions of spiral galaxies, and the global star formation history (S08; Fontanot et al. 2009; Kimm et al. 2009; Hopkins et al. 2009). With the addition of detailed chemical evolution modeling in Paper I, the model is able to match the mass–metallicity relation for galaxies and the trend of $[\alpha/\text{Fe}]$ with stellar mass, as well as the supernova rates as a function of specific star formation rate (SSFR). To achieve this agreement, it was necessary to adopt a Chabrier IMF (Chabrier 2003) with a slightly flatter slope above 1 M_\odot ($x = 1.15$ instead of $x = 1.3$), a relatively low fraction of binaries that yield a SN Ia event (0.03 in the $M = 3\text{--}16\text{ M}_\odot$ range), and a bimodal delay-time-distribution (DTD) with a prompt peak and a later plateau for type Ia supernovae (SNe Ia) explosions, as proposed by Mannucci et al. (2006). We will henceforth refer to the combined GCE plus SAM as the GCE-SAM.

Here we introduce two changes relative to the GCE-SAM described in Paper I. First, we have chosen a different set of yields for SNe Ia. Motivated by the excessive amount of Ni present in the galaxies and ISM in Paper I, we have switched from the yields of Nomoto et al. (1997, model W7) to those of Iwamoto et al. (1999, model WDD3) as the latter produces only half the Ni while the other elements remain approximately the same. The main difference between these SN models is the scenario for the explosion. The W7 model describes a slow deflagration of the stellar core, while the WDD3 model is calculated using a delayed detonation. The delayed detonation is also the currently favoured SNIa explosion scenario (see, e.g., de Plaa et al. 2007). The yields for SN II and AGB stars remain the same: Woosley & Weaver (1995, hereafter WW95) and Karakas & Lattanzio (2007), respectively.

The other change concerns the immediate fate of the metal-rich gas ejected by the stars. In the “standard” SAM of S08 (as in many SAMs, e.g. de Lucia et al. 2004), these metals were deposited directly in the ISM (cold gas phase

associated with the individual galaxy) where it is mixed instantaneously. However, this was a somewhat arbitrary choice. Perhaps a more physical scenario is that the ejecta from massive stars and supernovae is highly enriched, and it is this same material that escapes the galaxy and pollutes the ICM. This picture is supported by observations that indicate that galactic winds are ubiquitously metal-enriched (Martin 2005; Veilleux et al. 2005; Grimes et al. 2009; Weiner et al. 2009), as well as by hydrodynamic simulations of galactic outflows (Mac Low & Ferrara 1999; Madau et al. 2001; Scannapieco et al. 2008). We obtain good results when we assume that 80% of the new metals are deposited directly in the hot halo gas ($f_{\text{hot enrich}} = 0.8$). It is also interesting to note that Li et al. (2009) find that if 95% of the newly produced metals are ejected directly into the hot phase for galaxies with a DM halo mass of $5 \times 10^{10}\text{ M}_\odot$ or less, their semi-analytic model produces a good match for the mass function and metallicities of the Local Group dwarf satellite population. However, our results indicate that such a mass threshold is not necessary for reproducing the metal abundances in the ICM.

In this paper, we adopt a flat Λ CDM cosmology with $\Omega_0 = 0.28$, $\Omega_\Lambda = 0.72$, $h \equiv H_0/(100\text{ km s}^{-1}\text{ Mpc}^{-1}) = 0.701$, $\sigma_8 = 0.812$, and a cosmic baryon fraction of $f_b = 0.1658$, following the updated values of the cosmological parameters from Komatsu et al. (2009). We also leave the values of the free parameters associated with the galaxy formation model fixed to the fiducial values given in Paper I. We check that these parameters still produce good agreement with our calibration observations in the new “hot enrichment” models in Section 3.3.

3 RESULTS

In this section, we present our model results for the abundance ratios and metallicities of the ICM, as well as some basic properties of clusters, and compare them with a variety of observations. The simulations were run on a grid of haloes with virial mass ranging from $10^{14.25}\text{ M}_\odot$ to $10^{15.6}\text{ M}_\odot$ at an output redshift of $z = 0.05$. This value was chosen because it is the mean redshift of the groups and clusters in the observational samples.

3.1 Cluster masses, temperatures and gas fractions

In the observations, clusters are characterised by the measured spectroscopic X-ray temperature. In the models, the ICM temperature is taken to be equal to the halo virial temperature. Assuming isothermality, this temperature relates to the virial velocity as

$$T_{\text{vir}}[\text{keV}] = 35.9 k_B (V_{\text{vir}}[\text{km/s}])^2, \quad (1)$$

where k_B is the Boltzmann constant. At redshift $z = 0.05$, for the chosen cosmology, the previous formula translates to $T_{\text{vir}} = 4.12(M_{\text{vir}}/10^{15}\text{ M}_\odot)^{2/3}\text{ keV}$. The virial temperature is, however, systematically lower than the X-ray spectral temperature computed from the data (by typically 10%, Bower et al. 2008). This small correction should not pose an issue in the present work since the predicted and observed

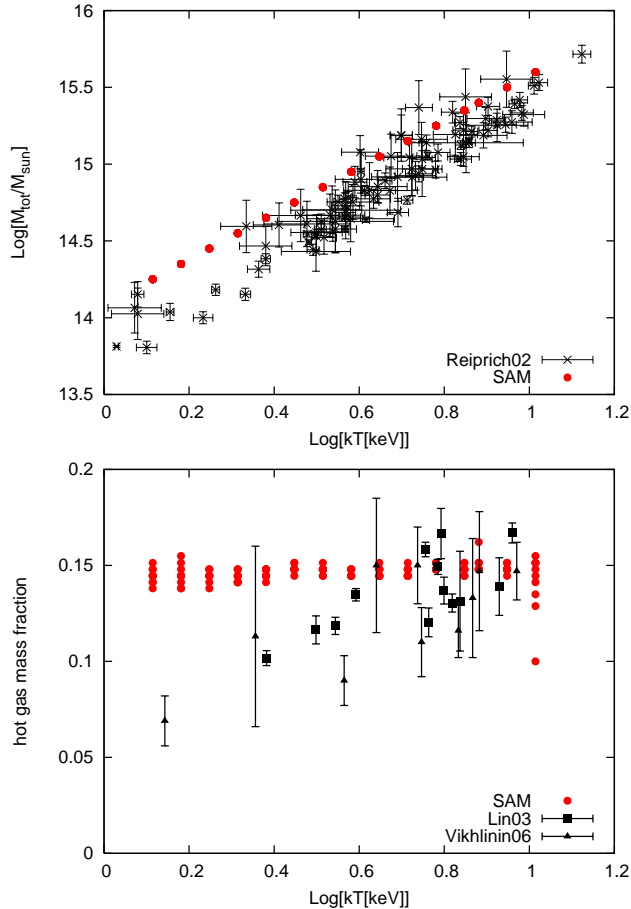


Figure 1. *Top:* The virial mass–temperature relation for large groups and clusters. Red circles: Model; black crosses: data points from Reiprich & Böhringer (2002). *Bottom:* The relation between the baryonic mass fraction and temperature. Red circles: Model; black triangles: data points from Vikhlinin et al. (2006); black squares: data points from Lin et al. (2003).

chemical properties of the ICM show an extremely flat dependence on cluster temperature.

Before looking into the metal abundances and ratios, we study the total mass and baryonic content of the simulated clusters. In Figure 1 we show the virial mass and the baryonic gas fraction of our simulated clusters as a function of temperature. The data points are taken from Reiprich & Böhringer (2002) for the total mass and Lin et al. (2003) and Vikhlinin et al. (2006) for the gas fraction. We do not show the models with “hot enrichment” here since this affects only the metal content and has a negligible effect on the total gas mass. In both cases, the models are in qualitative agreement with the data, albeit with some discrepancies. The small difference in the slope of the mass–temperature relation arises because real clusters are not strictly isothermal, as the models assume. Furthermore, correcting for the 10% systematic offset due to using the virial temperature rather than the X-ray temperature would bring the models into better agreement with the data. The hot gas fraction ($M_{\text{hot}}/M_{\text{vir}}$), however, shows no dependence with temperature over this range, unlike the data, which shows a mild trend of increasing baryonic frac-

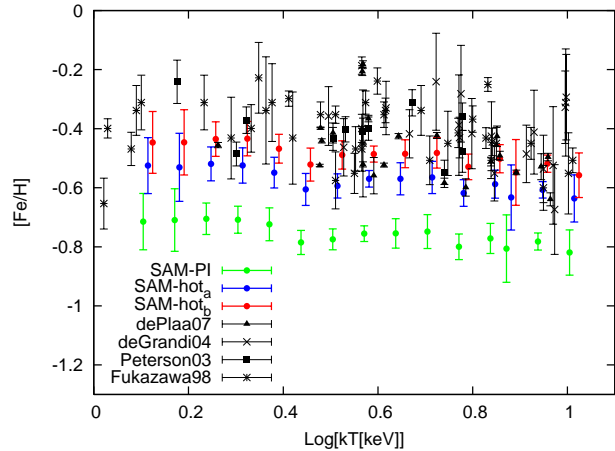


Figure 2. Iron abundance in the ICM as function of temperature. Green circles: Paper I fiducial model; blue and red circles: “hot enrichment” models with $A = 0.03$ and $A = 0.04$ respectively; black squares: data points from Peterson et al. (2003); black triangles: data points from de Plaa et al. (2007); black stars: data points from Fukazawa et al. (1998); black crosses: data points from De Grandi et al. (2004). The errorbars on the observational data represent uncertainties, while for the models they indicate the mean and 1σ dispersion over different halo realizations.

tion with temperature. This behavior was already seen in S08 (their Figure 8). Bower et al. (2008) have shown that if “radio mode” AGN feedback not only prevents the cooling of gas but is also allowed to eject some of the hot gas out of the halo, lower-mass clusters in the models will also show lower gas fractions. It is worth noting that our models agree well with the *mean* gas fraction of the entire data sample and that model haloes below 1 keV ($M_{\text{vir}} \sim 10^{12} M_{\odot}$) show a sudden drop in the predicted gas fraction (see S08 Figure 8). This step-like behaviour in the gas fraction is common to other models (De Lucia et al. 2004; Menci et al. 2006), and is due to the rapid transition from infall-limited cooling (sometimes called “cold mode”) to cooling-time limited cooling (“hot mode”).

3.2 Metallicities and abundance ratios

Our model proved in Paper I to be successful at reproducing the metallicity- and $[\alpha/\text{Fe}]$ -mass relations of local early-type galaxies, as well as the SN rates as a function of SSFR. We now examine the iron content and the abundance ratios between different elements and Fe in the ICM to further test its accuracy. We use an ensemble of X-ray cluster surveys for this purpose. From Fukazawa et al. (1998) we take Si and Fe; from Peterson et al. (2003) we take O, Ne, Mg, Si and Fe; from De Grandi et al. (2004) we take Fe (see also Ettori et al. 2002); and from de Plaa et al. (2007) we take Si, S, Ar, Ca, Fe and Ni. Galaxy clusters often show metallicity gradients for some elements, with increasing abundances towards the cluster centre. These clusters, known as *cool core* (CC) clusters, are mostly relaxed systems and the central metal enhancement is associated with feedback from the BCG. In contrast, *non-cool core* (NCC) clusters have almost flat abundance profiles and show signatures of recent merging events (De Grandi & Molendi 2001).

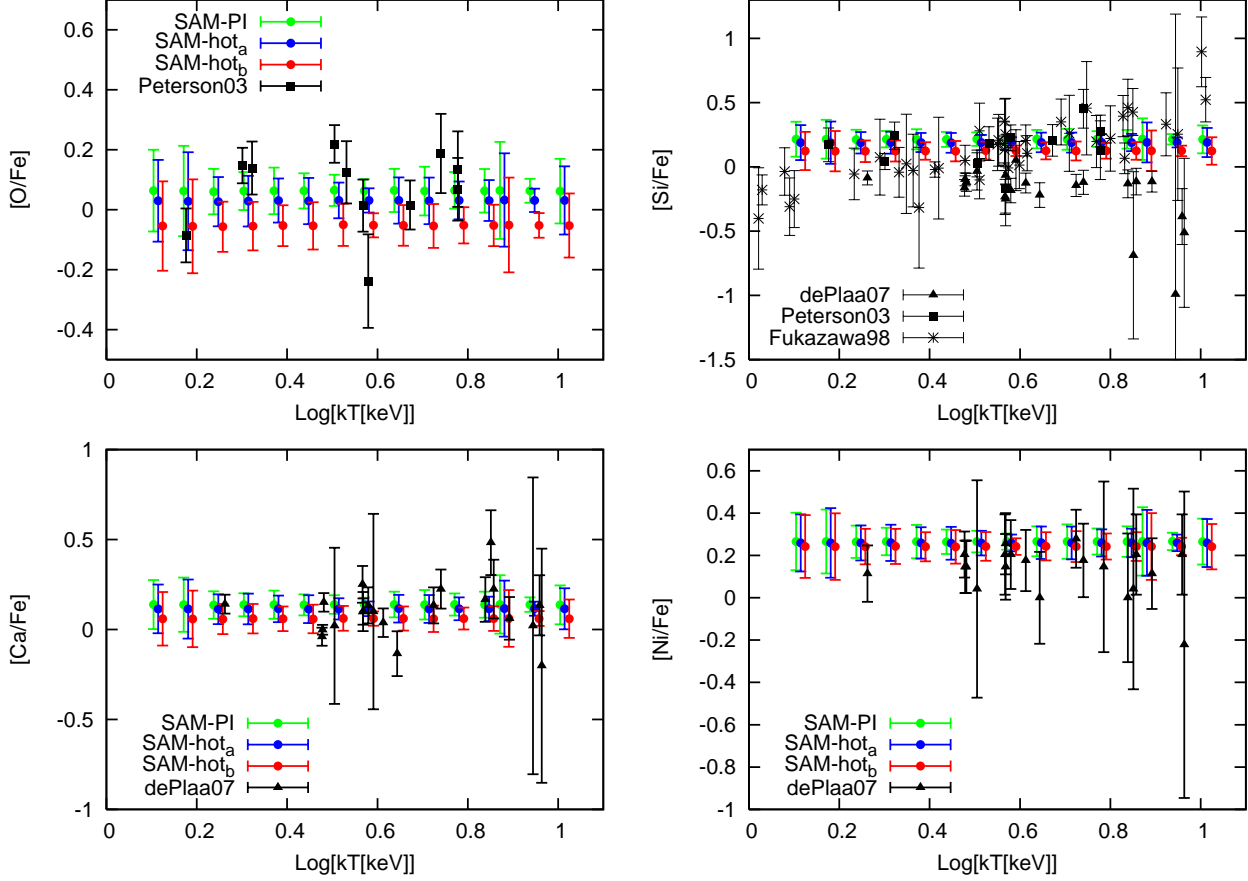


Figure 3. Abundance ratios in the ICM as function of temperature, for ratios matched well by the models. Clockwise from top left: [O/Fe], [Si/Fe], [Ni/Fe] and [Ca/Fe]. Symbols as in Figure 2. The errorbars on the observational data represent uncertainties, while for the models they indicate the mean and 1σ dispersion over different halo realizations.

Since the observational data are measured near the clusters centres and our models predict global abundances averaged over an entire cluster, it is necessary to correct the observations for gradients, but only for those clusters tagged as having *cool cores*. We do this by following the procedure of Nagashima et al. (2005a, Appendix A), who used the results of De Grandi et al. (2004) on Fe gradients to convert the measured central Fe abundance to global average values. Elements like Si, S, Ar, Ca and Ni are known to have the same gradients as Fe, and are corrected by the same factor. On the other hand, O, Ne and Mg do not show gradients even in CC clusters, so we assume that the global abundance is equal to the central measurement (Tamura et al. 2001, 2004). We have also renormalised the abundances to the solar values of Grevesse et al. (1996), as in the models.

In Figure 2, we examine the elemental abundance of iron ([Fe/H]). We pay particular attention to Fe because it is the ICM element most precisely measured and most extensively studied. Both the data and the models show a flat behaviour with temperature, an effect also seen in the abundance ratios (see below). It is clear that in the original model, the iron abundance is too low and inconsistent with the observations. Depositing the metals directly into the hot halo gas (hot enrichment) appears to be a plausible solution, bringing the models into marginal agreement with the data. In the models presented here, we have set the fraction of metals de-

posited directly into the ICM to 80% ($f_{\text{hot enrich}} = 0.8$). The metallicity of the hot gas depends weakly on this parameter, increasing by about a factor 1.5 over the full parameter range (zero to one). Therefore such a high value for $f_{\text{hot enrich}}$ is necessary to have a significant effect. In this sense, also, further increasing its value beyond $\simeq 0.75$ – 0.8 only raises the predicted abundances by a negligible amount. Another way to increase the iron content is by changing the number of type Ia supernovae by adjusting the parameter A , which sets the fraction of binaries that give rise to a SN Ia event. In Figure 2, we show results for both $A = 0.03$, the fiducial value adopted in Paper I (SAM – hot_a), and a slightly higher value, $A = 0.04$ (SAM – hot_b). We see that indeed, a higher fraction of type Ia SN binaries provides a better match to the ICM iron abundances, however the value of this parameter is constrained by the observed SN rates and can not take arbitrarily high or low values. As we show later, a binary fraction of 0.04 is still consistent with SNe Ia rates as a function of SSFR for galaxies in the local Universe while producing ICM [Fe/H] abundances that are in marginal agreement with the observed values.

In Figures 3 and 4 we show the abundance ratios of different elements to iron (O, Ne, Mg, Si, S, Ar, Ca and Ni) in models with and without “hot enrichment”. For those with “hot recycling” we again explore two different values for the SNIa binary fraction, $A = 0.03$ (SAM – hot_a) and $A = 0.04$

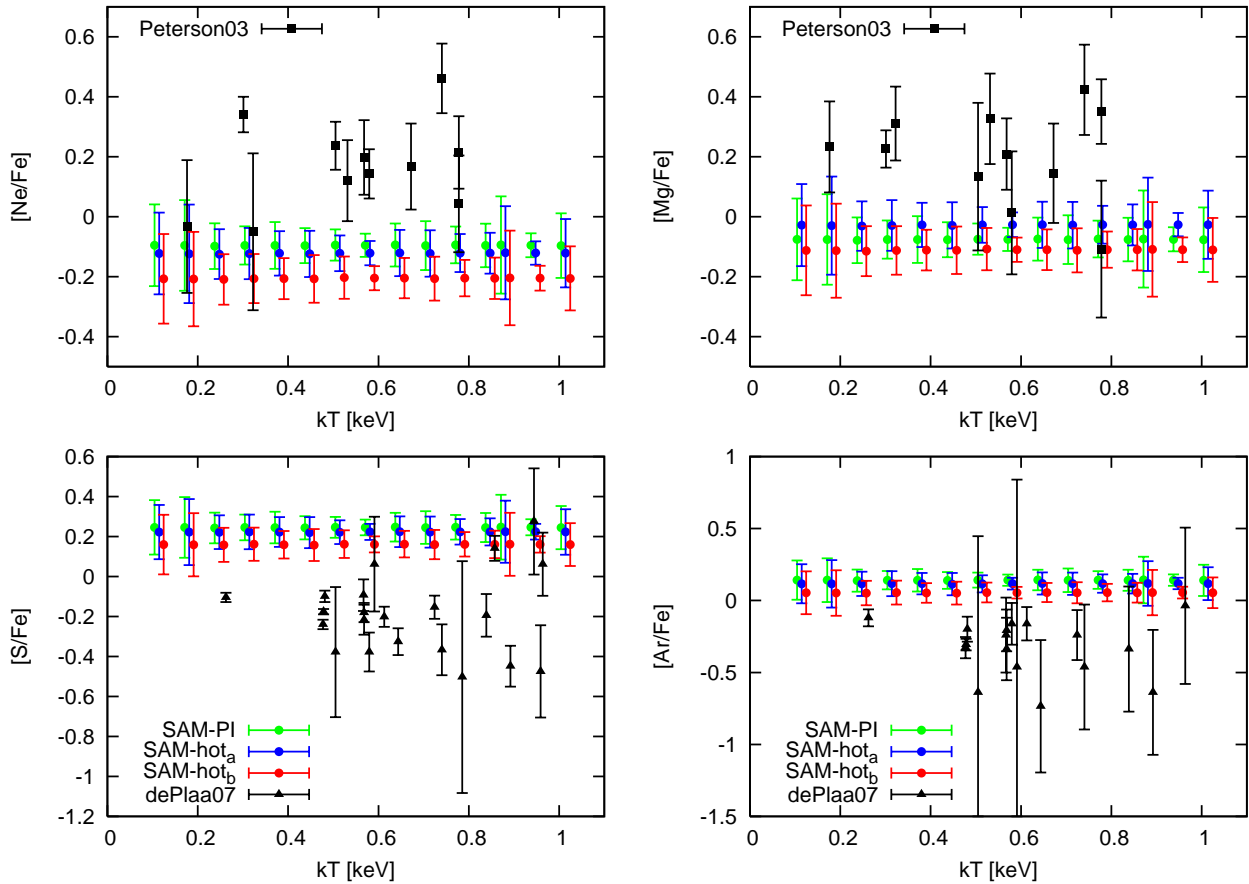


Figure 4. Abundance ratios in the ICM as function of temperature, for ratios matched poorly by the models. Clockwise from top left: $[\text{Ne}/\text{Fe}]$, $[\text{Mg}/\text{Fe}]$, $[\text{Ar}/\text{Fe}]$ and $[\text{S}/\text{Fe}]$. Symbols as in Figure 2. The errorbars on the observational data represent uncertainties, while for the models they indicate the mean and 1σ dispersion over different halo realizations.

(SAM – hot_b). There are two aspects that are common to all the elements. Firstly, models with hot enrichment show slightly lower abundance ratios than the standard model, especially for α elements. This is not surprising since the extra metals deposited by this mechanism come mainly from very low mass galaxies that have low values of $[\alpha/\text{Fe}]$. Secondly, all of the model abundance ratios show a flat behaviour with temperature, as does the data, although the zero point may disagree in some cases. Some of the ratios ($[\text{O}/\text{Fe}]$, $[\text{Si}/\text{Fe}]$, $[\text{Ca}/\text{Fe}]$ and $[\text{Ni}/\text{Fe}]$) show a very good match to the observations. On the other hand, the predicted values of $[\text{Mg}/\text{Fe}]$ and $[\text{Ne}/\text{Fe}]$ are too low, while $[\text{Ar}/\text{Fe}]$ and $[\text{S}/\text{Fe}]$ are over-predicted, although argon is marginally consistent with the data.

The effect of the higher SNIa binary fraction is naturally stronger on those elements produced mostly by SNIa. With the higher $[\text{Fe}/\text{H}]$ required for a consistent iron abundance, the ratios $[\text{Ne}/\text{Fe}]$ and $[\text{Mg}/\text{Fe}]$ are even lower and depart further from the observations. $[\text{O}/\text{Fe}]$ also decreases but is still consistent. $[\text{Ar}/\text{Fe}]$ and $[\text{S}/\text{Fe}]$ are closer to the data but are still overpredicted and only marginally consistent with the observations. $[\text{Si}/\text{Fe}]$ and $[\text{Ca}/\text{Fe}]$ remain in good agreement. Finally, $[\text{Ni}/\text{Fe}]$ shows no variation with the binary fraction parameter A , which is reassuring as both elements are predominantly produced by SNIa.

In the case of $[\text{Mg}/\text{Fe}]$, the model ratios can be raised

by increasing the Mg yield in stars above $20 M_{\odot}$, a common practice with the WW95 yields (see, e.g., François et al. 2004). In Paper I there was no need for such a modification, but in this case increasing the Mg yield by a factor of 2.5 brings the ICM abundance ratio into good agreement with the data, while still maintaining an observationally consistent $[\text{Mg}/\text{Fe}]$ in the galaxies’ stellar component. A slightly higher factor would give a better match for the ICM, but in that case the stellar abundance ratios would be too high. Models with a boosted magnesium yield are shown in Figure 5. In principle, the same exercise could be done with the yields of other elements that are underpredicted (Ne) or overpredicted (Si, Ar). However this should not be considered a solution, but simply a tentative constraint on nucleosynthesis from the chemical evolution models. Also, we have assumed that the different elements in the ICM either have no radial gradients at all or that they have the same gradient as iron (for which there are fairly good measurements). This simple assumption might not be strictly true and a more accurate correction for gradients could bring the models and the data into better agreement. Future observations of gradients of elements other than iron in the ICM would shed some light on this matter.

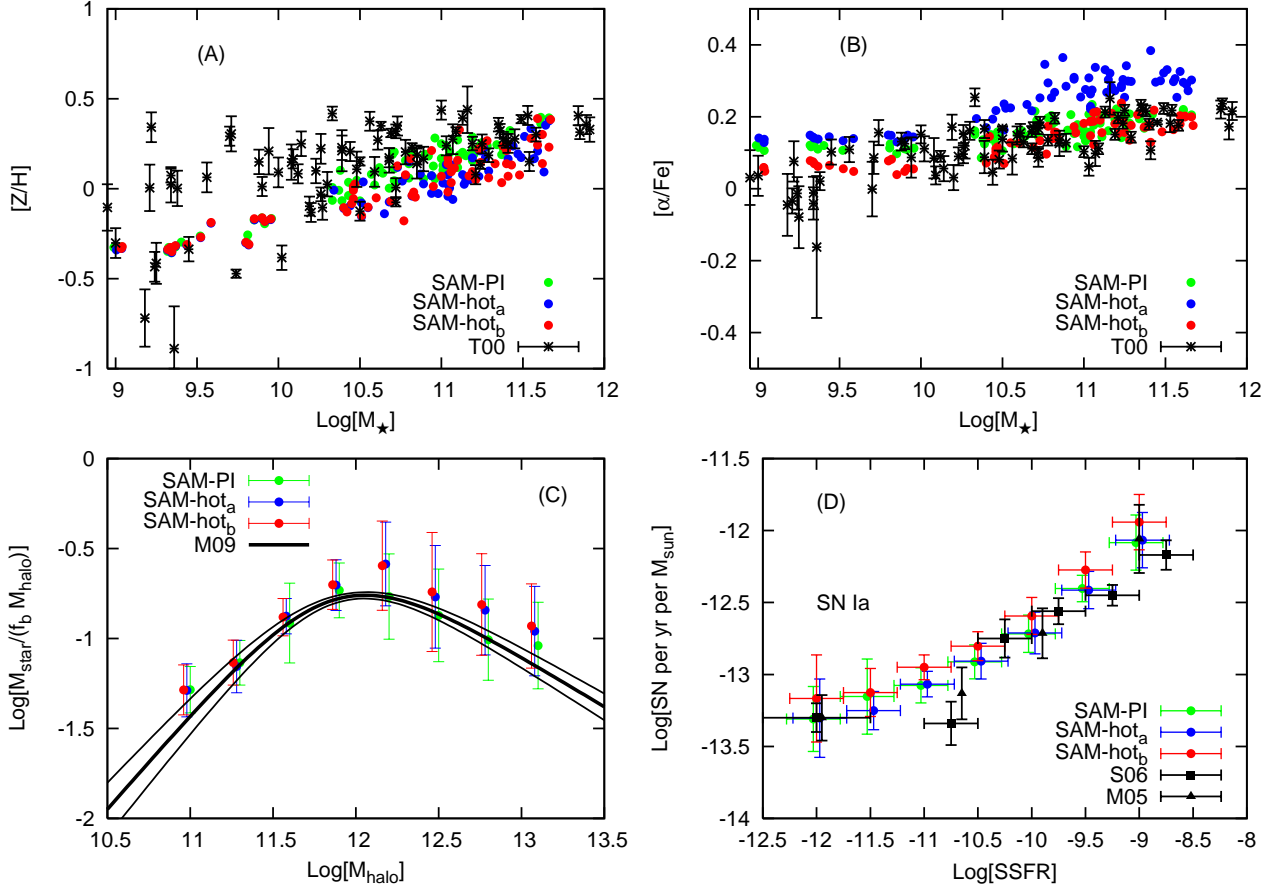


Figure 6. Predicted properties of galaxies in the local Universe. Clockwise, starting from the top left panel: (A) $[Z/H]$ vs. stellar mass for early-type galaxies; (B) $[\alpha/Fe]$ vs. stellar mass for early-type galaxies; (C) Fraction of baryons in the form of stars as a function of halo mass; (D) Type Ia SNR vs. SSFR. Symbols – green circles: Paper I fiducial model; blue and red circles: “hot enrichment” models with $A = 0.03$ and $A = 0.04$ respectively; T00: reanalysed metallicities and abundance ratios from Trager et al. (2000) as presented in Paper I; M05 and S06: SN rates from Mannucci et al. (2005) and Sullivan et al. (2006) respectively; M09: the empirical relation, and 1σ uncertainties, derived by Moster et al. (2009).

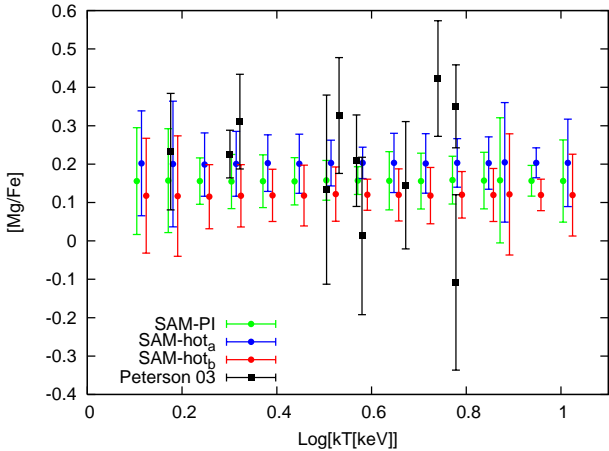


Figure 5. $[Mg/Fe]$ in the ICM as a function of temperature for models with the magnesium yield from SNII increased by a factor 2.5. Symbols as in Figure 2. The errorbars on the observational data represent uncertainties, while for the models they indicate the mean and 1σ dispersion over different halo realizations.

3.3 Effects of “hot enrichment” on galaxy properties

We have introduced a fairly significant modification to our model — the deposition of the majority of the newly produced metals into the hot halo gas, instead of into the cold interstellar gas. It is important to check whether this change has an impact on the properties of galaxies that we used to calibrate our previous models. In Figure 6 we show the same three models as in the previous section (Paper I fiducial, SAM-PI; hot enrichment with $A = 0.03$, SAM – hot_a; and hot recycling with $A = 0.04$, SAM – hot_b). We show the metallicity, $[\alpha/Fe]$ ratio, and SN Ia rate of galaxies, and compare them with the same data samples from the local Universe as in Paper I. We remind the reader that the fiducial model from Paper I had $A = 0.03$.

The metallicities of early-type galaxies are not significantly affected by this change and remain in agreement with the observations (panel A). However, galaxies in models with “hot enrichment” have their $[\alpha/Fe]$ increased (especially the most massive galaxies). A higher value of the binary fraction parameter A brings the abundance ratios back into agreement with the observations (panel B). From panel (D) in Figure 6, we see that the lower value of $A = 0.03$ provides a

better fit to the SN Ia rates as a function of the specific star formation rate (SSFR), although a value of $A = 0.04$ is still consistent with the data. Considering that a higher fraction of stars that explode as SNe Ia is also required to make the iron content in the ICM consistent with the data, $A = 0.04$ gives a better overall agreement between the models and the observations.

Another concern is that when metals are deposited directly into the hot gas, elevating the metal content, the cooling rate increases, possibly resulting in the conversion of a larger fraction of the baryons in the halo into stars. This could result in the production of an overabundance of massive galaxies relative to observations. We check this by investigating the ratio of the mass of baryons that have turned into stars in the central galaxy to the mass of baryons that would be contained in the halo in the absence of star formation or feedback (i.e. $f_b M_{\text{vir}}$, where f_b is the universal baryon fraction), as a function of halo mass. We compare the model predictions with the empirical constraint from Moster et al. (2009), which is derived by requiring that the observed stellar mass function is reproduced for a given assumed multiplicity function of dark matter halos (i.e. as predicted by a given Λ CDM model). As we can see from panel (C) in Figure 6, the effect of the new model ingredients is small and all models are consistent with each other and with the data.

4 DISCUSSION AND CONCLUSIONS

We have investigated the metal enrichment of the intracluster medium within the framework of hierarchical assembly using the same model presented in Paper I, which successfully reproduces the abundance ratios of early-type galaxies in the local Universe by assuming a slightly flat IMF ($x = 1.15$) and a bimodal Delay-Time-Distribution of type Ia supernovae.

Our most important finding is the need for some form of metal enriched outflows from galaxies because the ICM iron abundance is too low otherwise. Adopting “hot enrichment”, in which 80% of the metal-rich material ejected by the stars is deposited directly into the ICM rather than the ISM, seems to be a reasonable solution. We also need slightly more type Ia supernovae, both for the iron in the ICM and the $[\alpha/\text{Fe}]$ in the galaxies. Although the fit to SNR vs. SSFR is not as good as in Paper I, it is still consistent with the observations.

Regarding the elemental abundance ratios in the ICM, the models predict flat behaviour with cluster temperature, in agreement with the observations. For some elements (O, Si, Ca, Ni) the zero-point is reproduced remarkably well, while others agree only marginally (Ar, S), or are significantly underpredicted (Ne, Mg). This occurs irrespective of whether “hot enrichment” is assumed or not. The $[\text{Mg}/\text{Fe}]$ can be fixed by increasing the Mg yield in SN II (as is commonly done with the WW95 yields). The discrepancy in the other elements may arise from uncertainties in the yields and/or the correction for radial gradients (we assume that elements that have a gradient share the same one as Fe, which might not be strictly correct, although they cannot be too different).

Overall the model *simultaneously* produces acceptable

predictions for the chemical properties of galaxies in the local Universe and the ICM in nearby clusters. This is yet another step forward in building a self-consistent framework for predicting the properties of diverse populations within the context of the hierarchical galaxy formation framework.

ACKNOWLEDGEMENTS

We thank the directors of the Max-Planck-Institut für Astronomie, H.-W. Rix, and the Kapteyn Astronomical Institute, J.M. van der Hulst, and NOVA, the Lorentz Center and the Leids Kerkhoven-Bosscha Fonds for providing travel support and working space during the gestation of this paper. We also thank the Space Telescope Science Institute for travel funding and hospitality. We thank Y.S. Li and B.K. Gibson for helpful discussions.

REFERENCES

- Arrigoni M., Trager S. C., Somerville R. S., Gibson B. K., 2010, MNRAS, 402, 173
- Bower R. G., McCarthy I. G., Benson A. J., 2008, MNRAS, 390, 1399
- Chabrier G., 2003, PASP, 115, 763
- De Grandi S., Ettori S., Longhetti M., Molendi S., 2004, A&A, 419, 7
- De Grandi S., Molendi S., 2001, ApJ, 551, 153
- De Lucia G., Kauffmann G., White S. D. M., 2004, MNRAS, 349, 1101
- de Plaa J., Werner N., Bleeker J. A. M., Vink J., Kaastra J. S., Méndez M., 2007, A&A, 465, 345
- Ettori S., De Grandi S., Molendi S., 2002, A&A, 391, 841
- Fontanot F., De Lucia G., Monaco P., Somerville R. S., Santini P., 2009, MNRAS, 397, 1776
- François P., Matteucci F., Cayrel R., Spite M., Spite F., Chiappini C., 2004, A&A, 421, 613
- Fukazawa Y., Makishima K., Tamura T., Ezawa H., Xu H., Ikebe Y., Kikuchi K., Ohashi T., 1998, PASJ, 50, 187
- Gibson B. K., Matteucci F., 1997, MNRAS, 291, L8
- Grevesse N., Noels A., Sauval A. J., 1996, in Holt S. S., Sonneborn G., eds, Cosmic Abundances Vol. 99 of Astronomical Society of the Pacific Conference Series, Standard Abundances. pp 117–+
- Grimes J. P., Heckman T., Aloisi A., Calzetti D., Leitherer C., Martin C. L., Meurer G., Sembach K., Strickland D., 2009, ApJS, 181, 272
- Hopkins P. F., Somerville R. S., Cox T. J., Hernquist L., Jøge S., Keres D., Ma C., Robertson B., Stewart K., 2009, MNRAS, 397, 802
- Iwamoto K., Brachwitz F., Nomoto K., Kishimoto N., Umeda H., Hix W. R., Thielemann F.-K., 1999, ApJS, 125, 439
- Karakas A., Lattanzio J. C., 2007, Publications of the Astronomical Society of Australia, 24, 103
- Kimm T., et al., 2009, MNRAS, 394, 1131
- Komatsu E., et al., 2009, ApJS, 180, 330
- Li Y.-S., De Lucia G., Helmi A., 2009, MNRAS accepted
- Lin Y.-T., Mohr J. J., Stanford S. A., 2003, ApJ, 591, 749
- Mac Low M., Ferrara A., 1999, ApJ, 513, 142
- Madau P., Ferrara A., Rees M. J., 2001, ApJ, 555, 92

- Mannucci F., Della Valle M., Panagia N., 2006, MNRAS, 370, 773
- Mannucci F., Della Valle M., Panagia N., Cappellaro E., Cresci G., Maiolino R., Petrosian A., Turatto M., 2005, A&A, 433, 807
- Martin C. L., 2005, ApJ, 621, 227
- Matteucci F., Gibson B. K., 1995, A&A, 304, 11
- Menci N., Fontana A., Giallongo E., Grazian A., Salimbeni S., 2006, ApJ, 647, 753
- Moster B. P., Somerville R. S., Maubetsch C., van den Bosch F. C., Maccio' A. V., Naab T., Oser L., 2009, ArXiv e-prints
- Nagashima M., Lacey C. G., Baugh C. M., Frenk C. S., Cole S., 2005, MNRAS, 358, 1247
- Nagashima M., Lacey C. G., Okamoto T., Baugh C. M., Frenk C. S., Cole S., 2005, MNRAS, 363, L31
- Nomoto K., Iwamoto K., Nakasato N., Thielemann F.-K., Brachwitz F., Tsujimoto T., Kubo Y., Kishimoto N., 1997, Nuclear Physics A, 621, 467
- Peterson J. R., Kahn S. M., Paerels F. B. S., Kaastra J. S., Tamura T., Bleeker J. A. M., Ferrigno C., Jernigan J. G., 2003, ApJ, 590, 207
- Reiprich T. H., Böhringer H., 2002, ApJ, 567, 716
- Renzini A., 1997, ApJ, 488, 35
- Scannapieco C., Tissera P. B., White S. D. M., Springel V., 2008, MNRAS, 389, 1137
- Somerville R. S., Hopkins P. F., Cox T. J., Robertson B., Hernquist L., 2008, MNRAS, 391, 481
- Sullivan M., et al., 2006, ApJ, 648, 868
- Tamura T., Bleeker J. A. M., Kaastra J. S., Ferrigno C., Molendi S., 2001, A&A, 379, 107
- Tamura T., Kaastra J. S., den Herder J. W. A., Bleeker J. A. M., Peterson J. R., 2004, A&A, 420, 135
- Trager S. C., Faber S. M., Worthey G., González J. J., 2000, AJ, 119, 1645
- Veilleux S., Cecil G., Bland-Hawthorn J., 2005, ARA&A, 43, 769
- Vikhlinin A., Kravtsov A., Forman W., Jones C., Markevitch M., Murray S. S., Van Speybroeck L., 2006, ApJ, 640, 691
- Weiner B. J., Coil A. L., Prochaska J. X., Newman J. A., Cooper M. C., Bundy K., Conselice C. J., Dutton A. A., Faber S. M., Koo D. C., Lotz J. M., Rieke G. H., Rubin K. H. R., 2009, ApJ, 692, 187
- Woosley S. E., Weaver T. A., 1995, ApJS, 101, 181